

Manipulation of van der Waals forces to improve image resolution in atomic-force microscopy

Jeffrey L. Hutter and John Bechhoefer

Citation: [Journal of Applied Physics](#) **73**, 4123 (1993); doi: 10.1063/1.352845

View online: <http://dx.doi.org/10.1063/1.352845>

View Table of Contents: <http://scitation.aip.org/content/aip/journal/jap/73/9?ver=pdfcov>

Published by the [AIP Publishing](#)

Articles you may be interested in

[Application of the KolibriSensor® to combined atomic-resolution scanning tunneling microscopy and noncontact atomic-force microscopy imaging](#)

J. Vac. Sci. Technol. B **28**, C4E12 (2010); 10.1116/1.3430544

[Higher harmonics imaging in tapping-mode atomic-force microscopy](#)

Rev. Sci. Instrum. **74**, 5111 (2003); 10.1063/1.1626008

[Van der Waals and capacitive forces in atomic force microscopies](#)

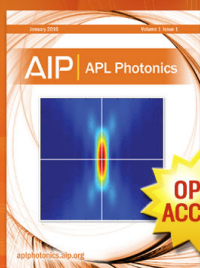
J. Appl. Phys. **86**, 5245 (1999); 10.1063/1.371506

[Measurement and manipulation of van der Waals forces in atomic-force microscopy](#)

J. Vac. Sci. Technol. B **12**, 2251 (1994); 10.1116/1.587752

[Van der Waals Forces in Atoms and Molecules](#)

J. Chem. Phys. **41**, 3955 (1964); 10.1063/1.1725842



Launching in 2016!

The future of applied photonics research is here

AIP | APL
Photonics

Manipulation of van der Waals forces to improve image resolution in atomic-force microscopy

Jeffrey L. Hutter and John Bechhoefer

Department of Physics, Simon Fraser University, Burnaby, British Columbia, V5A 1S6, Canada

(Received 9 October 1992; accepted for publication 7 January 1993)

Although the atomic force microscope (AFM) resembles superficially the scanning tunneling microscope (STM), its imaging resolution is in general much coarser. For the AFM, long-range interactions—most notably the van der Waals force—imply that image resolution is set by the macroscopic tip radius rather than by a single atom, as with the STM. Experimentally, we show that van der Waals forces can be measured using an AFM. By immersing tip and sample in an appropriate fluid, we can effectively eliminate the van der Waals force, leading to a marked improvement in AFM image quality.

I. INTRODUCTION

Imaging with atomic resolution requires a probe of atomic dimensions. This deceptively simple fact underlies the success of the scanning tunneling microscope¹ (STM), where the exponential decay of the electron tunneling current with tip-sample separation implies that only the region of the sample very close to the tip contributes to the current. Indeed, since the decay length of the tunneling current is approximately 1 Å, the total tunneling current will be dominated by electrons flowing through the single tip atom that is closest to the sample surface. Thus, although STM tips have a macroscopic radius of curvature at their ends—in practice rarely less than 100 Å—the effective tip size is nonetheless a single atom, enabling it to produce images that have atomic resolution. The chief limitation of the STM is that it requires conducting or semiconducting samples.

The atomic force microscope² (AFM) closely resembles the STM but obtains its topographical information from the short-ranged repulsion resulting from the overlap of electronic shells between tip and sample. If only short-ranged forces existed, the AFM would operate exactly as the STM does—through a single atom—and one would expect to achieve the same resolution (without the STM's restriction to conducting and semi-conducting surfaces). However, the presence of long-ranged interactions such as the van der Waals (vdW) force, leads to a very different imaging scenario in which the macroscopic tip radius controls the imaging resolution. The purpose of this paper is to explore in detail the undesired effects of long-ranged forces (in Sec. II and the Appendix) and to suggest a way to control those effects (in Sec. III). We report on experiments that show that vdW forces can be measured using an AFM in Sec. IV and that their deleterious effects on imaging may be largely eliminated.

II. ATOMIC FORCE IMAGING

We begin by considering the operation of an AFM in vacuum. The AFM uses a sharp tip mounted at the end of a cantilever spring to probe the surface of a sample. If the

tip and sample are electrically neutral, the tip will be subject to three forces: a spring force due to the cantilever, a short-ranged repulsive contact force, and a long-ranged attractive van der Waals force.

The short-ranged repulsion is usually modeled by one of the following three potentials:³ a hard-sphere potential,

$$w(r) = \begin{cases} 0 & \text{for } r \geq r_0 \\ \infty & \text{for } r < r_0 \end{cases} \quad (1a)$$

where r_0 is the hard-sphere diameter, a power-law potential,

$$w(r) = (c/r)^n, \quad (1b)$$

where n is often chosen to be 12, or an exponential potential,

$$w(r) = ce^{-r/r_0}, \quad (1c)$$

with a value of about 0.2 Å assigned to the parameter r_0 . In fact, the exact form of this potential matters little, save that it be short-ranged.

The van der Waals (vdW) potential between two molecules, being the result of induced dipole – induced dipole interactions, has the familiar $-C/r^6$ form. In order to calculate the force between a spherical tip of radius R and a flat surface, one may use a continuum approach and integrate the $1/r^6$ interaction over the volume of the tip and surface.⁴ The result is that, for small distances, the potential has the approximate form

$$W(D) = -\frac{AR}{6D}, \quad D \ll R, \quad (2)$$

where D is the separation between the sphere and surface, and $A \equiv \pi^2 C \rho_1 \rho_2$ is the so-called Hamaker constant, where ρ_1 and ρ_2 are the densities of the two solids.

In Fig. 1, we show a simple model of AFM operation. The cantilever is represented by a spring of force constant k . (The value of k will depend, of course, on the elastic moduli of the cantilever material as well as on the cantilever geometry.⁵ Typical values range between 0.03 and 0.5 N/m.) The tip is represented by a sphere of radius R ,

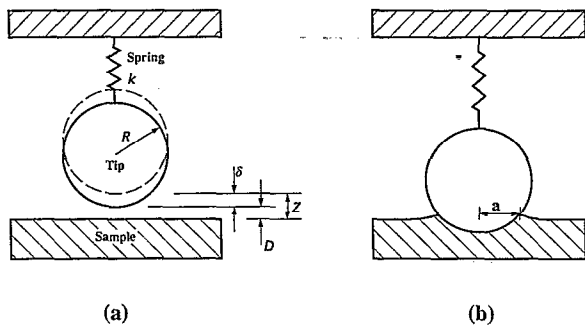


FIG. 1. Simple model for the tip-surface interaction. (a) A tip of radius R is suspended a distance D above a surface. The tip is acted on by vdW forces, causing the spring to stretch and the tip to move by an amount δ from the spring equilibrium height Z above the sample. Note that in the case of an attractive vdW interaction, shown here, δ is negative. (b) The snapping instability causes the tip to hit the sample. Finite elastic moduli cause the tip and sample to deform. As suggested here, the sample is usually softer than the tip and deforms more.

although the actual geometry is more complicated. (Our tips are nominally four-sided pyramids ending in a rounded tip with a radius of about 500 Å.) We may ignore the details of the tip geometry because the vdW forces are dominated by the atoms of the tip that are closest to the sample. (In AFM imaging, the distance between the surfaces is small compared to the radius of curvature of the tip.) Moreover, the effective range of the van der Waals forces is limited to several hundred angstroms by retardation effects:⁶ the finite speed of light limits the distance over which an induced dipole can interact with the fluctuating dipole that induced it. Thus, we may ignore the contribution to the vdW force from atoms that lie outside the ball at the end of the tip. In Fig. 1(a), Z is the height of the bottom of the tip above the surface in the absence of external forces. The short- and long-ranged forces acting on the tip will cause a deflection, δ , from the equilibrium height Z . Thus, the actual separation between the tip and sample is $D = Z + \delta$.

Ordinarily, the cantilever is fixed and the sample displaced by a piezoelectric tube scanner capable of lateral (x, y) and vertical (z) motions. As the sample scans beneath the tip, the cantilever bobs up and down in response to forces acting between tip and sample. The deflection is measured (by the optical-lever technique,⁷ in our case) and used to generate a topographic map of the surface. For imaging, a feedback circuit may be used to control the z extension of the scanner to maintain a constant tip deflection. The voltage applied to the z plates on the piezoelectric tube at each point of the region imaged is then related to the height of the sample at that point.

During AFM operation, one must begin with the tip far from the sample and extend the piezo until the tip is close enough to have a measurable interaction with the sample. As the tip approaches the sample, the vdW attraction will cause the cantilever to deflect, as in Fig. 1(a). Imaging may be performed when the tip and sample are not in contact,^{8,9} but the resolution is limited to scales on the order of the tip-sample separation.

In the absence of the short-ranged repulsion, the equilibrium tip position will be one where the vdW and spring forces balance. This point may be determined by finding the energy minimum for the system. The potential energy may be written as

$$E(\delta, Z) = -\frac{AR}{6(Z+\delta)} + \frac{1}{2}k\delta^2, \quad (3)$$

where Z is determined by the piezo extension and acts as a control parameter. This energy function has a singularity at $\delta = -Z$, when the tip-sample distance is zero. Of course, contact forces will always limit the approach distance to a few angstroms. Local minima of the energy function may be found by setting its derivative equal to zero:

$$\frac{dE(\delta, Z)}{d\delta} = \frac{AR}{6(Z+\delta)^2} + k\delta = 0. \quad (4)$$

Thus, the critical values of E are the solutions of a cubic equation and so can be calculated analytically. Note that Eqs. (3) and (4) may be scaled so that they depend on only one parameter, $\ell \equiv \sqrt[3]{AR/k}$, which is the length scale at which the vdW forces are able to deflect the spring significantly.

For large tip-sample distances, the cantilever feels no forces and $\delta=0$. As Z is decreased, moving the tip and sample together, an attractive vdW interaction ($A > 0$) will cause the tip to be deflected toward the sample. The equilibrium tip position in our model is a local minimum of Eq. (3). Solving Eq. (4) for δ , we find that when Z is decreased to $3^{2/3}\ell/2$, the solution corresponding to the slightly deflected tip becomes unstable — the magnitude of the gradient in the vdW force has become larger than that in the spring force.¹⁰ At this point, cantilever deflection will have brought the tip to a distance of $D = Z + \delta = 2Z/3 = \ell/\sqrt[3]{3}$ from the sample. The tip must then “snap” into contact with the surface. For typical values of the Hamaker constant, tip radius, and spring constant (10^{-19} J, 500 Å, and 0.1 N/m, respectively), the tip will jump into contact with the surface when it is about 26 Å away. This separation is still large enough that atomic-scale roughness will have a negligible effect on determining the tip deflection and snapping point. Conversely, the tip-sample distance at the snapping point is considerably less than the tip radius, so the assumption in Eq. (2) that $D \ll R$ in the region of interest is justified.

Once the tip and sample are in contact, the short-ranged forces may be used to image the surface of the sample. This is the standard mode of operation for the AFM. The tip is then at a position where the net force due to the spring and the large vdW interaction is balanced by the repulsion from the relatively few tip atoms in contact with the sample. In vacuum, the vdW forces are large enough that deformation of the tip and the sample is inevitable.¹¹

If the sphere and surface were infinitely rigid, they would touch at just one point. Because each body has a

finite elastic modulus, they each deform and make contact over a small circle of radius a_0 . This situation is illustrated in Fig. 1(b). The size of this circle for an external loading force was calculated long ago by Hertz.¹² Here, the loading force is caused by the vdW interaction between the bodies themselves (as well as by any additional spring force). In this case, the contact area is increased as the vdW attraction deforms the surfaces, bringing a larger area into contact.¹³ Expressions for the contact radii for these two cases have been included in the Appendix.

As the AFM exploits the short-ranged repulsion of the sample to map out a surface, it is clear that the resolution of the AFM is determined by the area of contact between the tip and sample. Since the vdW force between the two surfaces causes them to snap into contact, the contact area will have a value determined by the vdW force between the two surfaces at the closest distance allowed by the short-range repulsion. For typical values of the Hamaker constant ($\sim 10^{-19}$ J for the silicon nitride-mica system, which is used in this experiment), and assuming that the distance D_0 will be determined by the covalent radii of the atoms on the surface of the tip and sample ($D_0 \sim 1.5$ Å for surface oxygen atoms on the mica in contact with nitrogen atoms of the tip), the contact radius will be about 33 Å. (See the Appendix for details.)

One might think that some of the vdW attraction could be balanced by using the spring to pull up on the tip. However, once the two surfaces have been pressed into contact, the vdW forces will cause them to adhere with a finite contact area even if the loading force is subsequently reduced to zero, as explained in the Appendix. Thus, a finite force is required to pull the two surfaces apart. For the example cited above, the contact radius would only decrease from about 33 Å to about 21 Å before separation occurs.

Clearly, these contact radii are too large to allow atomic resolution. It is still possible to image the surface of an ordered material, but the image will be a moiré pattern resulting from the interaction between the lattices of both tip and sample. Lattice constants can be measured from such images, but local features will not be resolved. Such “moiré images” are characterized by perfect lattices with no local defects. On the other hand, when the AFM has been used to image non-periodic structures, such as DNA,¹⁴ the resolution does not exceed 30–50 Å.

As indicated in Eq. (A9), the characteristic resolution scale \mathcal{R} of contact-mode AFM imaging depends on the Hamaker constant and tip radius as

$$\mathcal{R} = \left(\frac{AR^2}{8KD_0^2} \right)^{1/3}, \quad (5)$$

where $1/K$ is the function of the elastic properties of the tip and sample defined in the Appendix (K is approximately equal to the smaller of the Young's moduli of the tip and sample). Though our discussion of resolution in terms of continuum mechanics must break down as \mathcal{R} approaches atomic scales, the vdW forces must be smaller than 1 nN for such a small \mathcal{R} (see the Appendix). Various studies have discussed the limits of AFM resolution at the atomic level in terms of the interaction between a sample and a single-atom tip. It is generally found that atomic resolution is possible if the contact force can be kept small enough (< 5 nN).¹⁵ Thus, Eq. (5) should be a reasonable form for the resolution down to atomic scales.

Under typical conditions, the resolution \mathcal{R} is at least 20 Å and in practice is often larger. The relationship between AFM resolution and an attractive vdW force described by Eq. (5) is well-known¹⁶ and suggests two strategies for improving AFM resolution. The most obvious one is to decrease the effective tip radius. As stated, our tips have a radius of about 500 Å.¹⁷ Various “supertips” with nominal radii as low as 100 Å have been developed recently. Standard AFM tips have also been sharpened to about 100 Å by deposition of material and by ion milling. A second strategy to improve imaging, which is pursued here, is to modify the Hamaker constant itself. As we shall see in Sec. III, this may be done by immersing tip and sample in a liquid medium. This approach has been suggested for noncontact AFM studies.¹⁸

III. MANIPULATION OF THE HAMAKER CONSTANT

The calculation of the vdW force in Sec. II was between a tip and sample separated by vacuum. The form given by Eq. (2) ignores many-body effects, the effect of an intervening liquid medium, and retardation effects for large distances. When the first two effects are taken into account, the form of the interaction potential is unaltered; the only change is in the value of the Hamaker constant. As mentioned above, retardation is only important at much larger tip-sample separations than are relevant for the AFM. In the non-retarded limit, the Hamaker constant between two media with a third intervening medium can be calculated using the Lifshitz theory.¹⁹

Although Lifshitz theory gives an exact formula for the Hamaker constant, that expression requires a representation of the dielectric responses of the media involved up to ultraviolet frequencies.^{20,21} For the purposes of this paper, it is sufficient to consider an approximate form for the Hamaker constant due to Israelachvili.²²

$$A_{132} = \frac{3}{4} k_B T \left(\frac{\epsilon_1 - \epsilon_3}{\epsilon_1 + \epsilon_3} \right) \left(\frac{\epsilon_2 - \epsilon_3}{\epsilon_2 + \epsilon_3} \right) + \frac{3h\nu_e}{8\sqrt{2}} \frac{(n_1^2 - n_3^2)(n_2^2 - n_3^2)}{(n_1^2 + n_3^2)^{1/2}(n_2^2 + n_3^2)^{1/2}[(n_1^2 + n_3^2)^{1/2} + (n_2^2 + n_3^2)^{1/2}]}, \quad (6)$$

where the ϵ_i 's are the static dielectric constants and the n_i 's are the optical refraction indices of the tip (1), sample (2), and immersion medium (3). In Eq. (6), ν_e is the electronic absorption frequency, which is assumed to be equal for all three media. Although approximate, Eq. (6) is valuable in that it highlights the roles of relative refraction indices and (to a lesser extent) dielectric constants in determining the value of A_{132} .

It is clear from Eq. (6) that Hamaker constants need not be positive. If the intervening medium has dielectric properties intermediate to those of the tip and sample, A_{132} will be negative, corresponding to repulsive van der Waals forces. This simply reflects the fact that one surface may attract the opposite surface less strongly than it does the intervening medium, resulting in a net repulsion between the bodies. A similar effect, dependent on the density of the materials involved, occurs when a wooden ball floats upwards in water: the gravitational interaction between the ball and the Earth is repulsive in the presence of a water medium.

If the Hamaker constant can be made negative, it can also — by appropriate choice of liquid medium — be made zero, or at least very small. By choosing a liquid for which the vdW interactions are repulsive, we avoid the snapping instability. This allows us to choose the applied force, rather than having it be set by adhesion forces, as is usually the case when attractive vdW interactions are present. The resolution will then no longer be given by Eq. (5), but will instead depend on the area of the tip brought into contact with the sample by an applied spring force. In addition, the natural surface roughness of the tip can then give rise to true atomic resolution in the same manner as the STM. The first priority, then, is to have a purely repulsive interaction. Given a repulsive interaction, the weaker it is the better, so as to minimize deformation of the surface when the tip is moved closer to the sample.

IV. EXPERIMENTAL

Our goal, then, was to find a liquid medium for which vdW interactions between tip and sample were repulsive and weak. To proceed, we measured deflection versus piezo extension curves for a collection of Si_3N_4 tips and muscovite mica samples immersed in various media. To prevent contamination, a new mica sample was used for each different medium. This sample was fixed in a liquid cell, which allows operation of an AFM with both tip and sample immersed, and cleaved after immersion in the medium to be studied. (Mica cleaved in air is rapidly coated by a thin film of water.) Tips were rinsed in the immersion medium for an hour before use. In addition, at least one new tip was used for each medium.

Deflection versus piezo extension curves are often called force spectra since the cantilever deflection is proportional to the spring force acting on the tip. They are measured by extending and withdrawing the piezo scanner through part of its vertical range. Measurements were made with a commercial atomic force microscope¹⁷ using a modified version of the force-spectrum routine to acquire 4096 points per spectrum. Ordinarily, such routines aver-

age the force spectra over several cycles. We found, however, that small thermal drifts, which can be caused by evaporation of the medium as well as by overall temperature fluctuations in the experimental apparatus, cause an offset of the curves in successive cycles, smearing out the information contained in the narrow range where vdW forces can be seen to act. For this reason, single-cycle force spectra were recorded and values of the force parameters were averaged after extraction. The approach speed was set to 1400 Å/s, which is slow enough that viscosity effects are unimportant,²³ except for very viscous fluids, yet fast enough that drift in the electronics and temperature is not a problem. Up to thirty spectra were recorded for each tip-medium combination.

We used cantilevers with low spring constants to increase the deflection caused by the forces. Since these cantilevers are longer than those with higher spring constants (200 μm as opposed to 100 μm), they are also better able to endure repeatedly being pressed through several thousand angstroms in contact with the surface. The cantilevers used had theoretical spring constants of 0.032 and 0.064 N/m.¹⁷

Equation (6) suggests that in order to minimize the vdW interaction, we should choose a medium with a dielectric constant and a refractive index close to those of either the tip or the sample. Since both mica and Si_3N_4 have rather high refractive indices (1.574 and 1.986, respectively^{24,25}), very few liquids meet these criteria. The dielectric constants of mica and Si_3N_4 are 5.4 and 6.34, respectively.^{26,25} For this study, three liquids were chosen: ethanol (which has a refractive index of $n_D = 1.3594$ and a dielectric constant of $\epsilon_0 = 24.55$), 1-bromonaphthalene ($n_D = 1.6582$, $\epsilon_0 = 5.12$), and 1-methylnaphthalene ($n_D = 1.6170$, $\epsilon_0 \sim 5$).^{27,28} Equation (6) indicates that the vdW interaction should be attractive, repulsive, and small, respectively.

Figure 2 shows representative experimental curves for the three media. These curves indicate the tip deflection as the tip *approaches* the sample. We did not use the curves for tip withdrawal since adhesion forces depend on the contact area between tip and sample, which varies from run to run.

We note that the vdW interaction is strongly attractive in the case of ethanol, as one would expect. Both other liquids give a repulsive interaction. The interaction for 1-bromonaphthalene is smaller than that for 1-methylnaphthalene. The reverse ordering for the naphthalene derivatives is not very worrisome: these liquids have dielectric properties similar to that of mica, so that small errors in the dielectric data can change the sign of the predicted Hamaker constant. In fact, more accurate calculations based on the Lifshitz theory predict that the interactions will be attractive in all three cases. Even these predictions must be treated with care, for they are only as precise as the dielectric data used as input. In particular, good data for mica is difficult to obtain as the physical properties vary from sample to sample. The overall difference between the results for ethanol and those for the

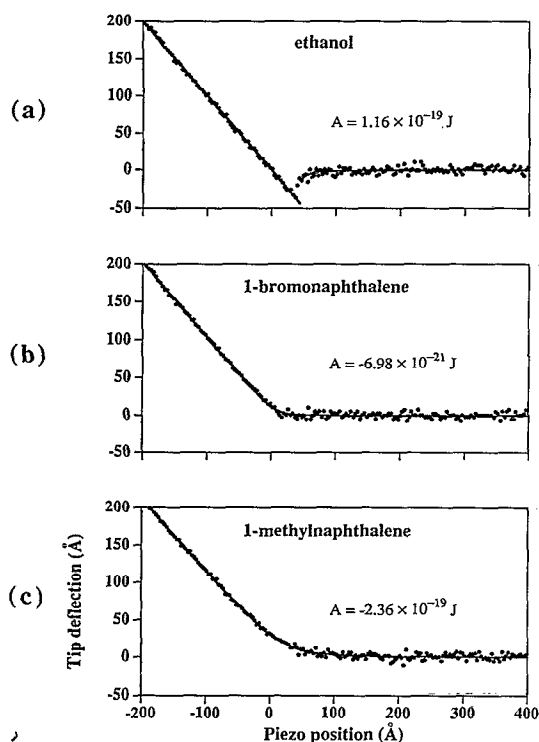


FIG. 2. Representative deflection vs piezo extension curves for a Si_3N_4 tip interacting with a mica sample across various media. The data have been scaled so that the x-axis gives Z , the distance between the sample and the undeflected tip position. Solid curves are theoretical fits to the data. In each case, the value of the Hamaker constant, A , has been calculated from the fitting parameter $\ell \equiv \sqrt[3]{AR/k}$ for the plot, assuming the nominal values for R and k . (a) Attractive interaction in ethanol ($\ell = 44.9 \text{ \AA}$). (b) Small repulsive interaction in 1-bromonaphthalene ($\ell = -22.2 \text{ \AA}$). (c) Repulsive interaction in 1-methylnaphthalene ($\ell = -56.9 \text{ \AA}$).

naphthalenes is nonetheless in agreement with expectations based on Eq. (6).

We can use the force spectra to estimate the strength of the vdW interaction. The most convenient method for attractive interactions is to simply measure the size of the jump to contact. In order to do this, one needs to be able to calibrate the vertical axis of the force spectrum. This is easily done by assuming that when the tip and sample are in contact, changes in the piezo height must result in equal changes in the tip deflection. (We assume that the compliance of the cantilever is smaller than those of the tip and sample. This has been tested in other studies where cantilevers with much larger force constants were used.²⁹) Solving Eq. (4) for $\delta(Z)$, reveals that the Hamaker constant can be calculated as

$$A = \frac{3k\Delta_+^3}{R}, \quad (7)$$

where Δ_+ is the snapping distance. For repulsive interactions, we can simply measure the tip deflection at $Z=0$. The $Z=0$ position may be located by finding the intersection between the baseline for the undeflected tip and the line asymptotic to the force spectrum when the tip and sample are in contact. We then find

$$A = \frac{6k\Delta_-^3}{R}, \quad (8)$$

where Δ_- is the measured deflection. A better procedure, which we have implemented as well, is to fit the full force spectrum curve using predictions based on Eq. (3). The full fit was used to calculate the solid lines shown in Fig. 2. For this paper, the values of Hamaker constants were used only to quantify the attraction or repulsion measured with the force spectra. Elsewhere, we give full details concerning the fitting procedure and focus on the use of the AFM as a means of making local measurements of Hamaker constants.³⁰

Preliminary images of mica indicate that image contrast does improve when a repulsive medium is used. Of course, a better demonstration of image quality would be to compare images of a step, defect, or adsorbed molecule produced with different media. However, a clear improvement in resolution of DNA strands was observed by Hansma *et al.* upon imaging in 1-propanol compared with images taken in ethanol.¹⁴ Propanol, unlike ethanol, leads to a slightly repulsive force spectrum reminiscent of our Fig. 2(b). Curiously, both Eq. (6) and the more exact Lifshitz theory predict that the vdW interaction should be attractive for propanol. Indeed, the Hamaker constant should be only marginally smaller than for ethanol. We believe that in this case, a force other than the vdW interaction — the solvation force³¹ — is at play. We discuss this in detail elsewhere.³⁰ But whatever the origins, a small repulsive force does lead to better image resolution.

V. CONCLUSIONS

The resolution of an AFM operated in contact mode is set by the contact area between the tip and sample. Attractive van der Waals forces cause a mechanical instability that snaps the tip into contact with the sample, leading to elastic deformation and a finite contact area. The size of this contact area depends on the macroscopic tip size.

In order to improve AFM resolution when attractive vdW forces operate, there are two strategies: decrease the tip radius R (make the tip sharper) or decrease the Hamaker constant A (reduce the long-ranged forces). In this paper, we have pursued the latter strategy. A further step clearly would be to combine the strategies. We note that the relatively high value of the index of refraction for silicon nitride will lead to a large van der Waals force whatever the choice of liquid medium. Thus, a related strategy is to try to find a tip material that will minimize the tip's contributions to A . It is clear that such a tip material will have to be an insulator rather than a metal or semiconductor.

Since Eq. (5) only holds for attractive vdW forces, yet another strategy is possible. The dependence of the contact area on the vdW force can be eliminated by setting the Hamaker constant to zero. The contact area is then controlled by the externally applied spring force.

We have shown experimentally that both attractive and repulsive vdW interactions can be measured using the AFM. This has important implications for image resolu-

tion and raises the possibility of using the AFM to map out local variations of the Hamaker constant.³² And most importantly, we have shown that by careful choice of an immersion medium, long-ranged forces may be eliminated, allowing the AFM to operate using the short-ranged repulsion between the sample and a single-atom tip.

ACKNOWLEDGMENTS

We thank J. N. Israelachvili for helpful suggestions. The AFM used in this study was purchased with an equipment grant from the Natural Sciences and Engineering Research Council of Canada (NSERC). The research was supported also by an operating grant from NSERC. J. H. acknowledges funding from a President's Research Grant from Simon Fraser University.

APPENDIX: CALCULATION OF TIP-SAMPLE DEFORMATION

Elastic deformation will occur whenever two bodies are in contact. Consider a sphere of radius R which is pressed by a loading force F into contact with a flat surface. Macroscopic deformation in the absence of surface forces may be estimated using the Hertz theory.¹² The region of contact in such a case will have a radius a_H given by

$$a_H^3 = \frac{RF}{K}, \quad (A1)$$

where $1/K$ is given by

$$\frac{1}{K} = \frac{3}{4} \left(\frac{1-\nu_1^2}{E_1} + \frac{1-\nu_2^2}{E_2} \right), \quad (A2)$$

where ν is Poisson's ratio and E is Young's modulus for materials 1 and 2 (tip and sample).

This theory may be used to estimate the maximum loading force permitted for atomic resolution. For typical values of the Young's modulus (1.5×10^{11} N/m² for Si₃N₄), Hertz theory predicts that in order to have a contact radius of 5 Å between a sample and a tip with a 500 Å radius of curvature, the loading force may not exceed 0.3 nN. This force is considerably smaller than the vdW force between the tip and sample in cases relevant to AFM operation in air. If we continue to approximate our deformed tip as a sphere, the force between it and the sample may be calculated by differentiating Eq. (2) with respect to D :

$$F = \frac{AR}{6D_0^2}, \quad (A3)$$

where D_0 is the minimum distance between sphere and surface allowed by the repulsive contact forces. Equation (A3) gives a value of 37 nN for the system discussed above, assuming values of 10^{-19} J for A and 1.5 Å for D_0 . The true force will, in fact, be greater because of the contact area between the deformed sample and the flattened tip.

While the Hertz theory may provide a sufficiently accurate model for the case of repulsive vdW forces,³³ the

actual contact area will be underestimated if attractive forces act. For the case of adhesion between the surfaces, a more exact calculation yields the formula¹³

$$a^3 = \frac{R}{K} [F + 3\pi R W_{12} + \sqrt{6\pi R W_{12} F + (3\pi R W_{12})^2}] \quad (A4)$$

for the radius a of the contact region between a sphere of radius R and a plane. In Eq. (A4), F is the external loading force and W_{12} is the adhesion energy, which here is due to the van der Waals interaction. In the absence of an external load, the contact radius remains finite and is given by

$$a_0 = (6\pi R^2 W_{12}/K)^{1/3}. \quad (A5)$$

Adhesion causes the surfaces to remain in contact, even with small negative loads, until a critical value, given by

$$F = -3\pi R W_{12}/2, \quad (A6)$$

when the value of a given by Eq. (A4) becomes complex. At this point, the contact area abruptly goes to zero as the surfaces detach. The minimum radius reached before separation is given by

$$a_{\min} = (3\pi R^2 W_{12}/2K)^{1/3} = a_0/4^{1/3}. \quad (A7)$$

To estimate the adhesion energy, we assume that the tip and sample surfaces are flat over the region of interest. Then the energy per unit area required to separate the surfaces is³⁴

$$W_{12} = A/12\pi D_0^2. \quad (A8)$$

Combining Eqs. (A7) and (A8), we see that the minimum radius \mathcal{R} of the contact area of a sphere and surface is given by

$$\mathcal{R} = \left(\frac{R^2 A}{8K D_0^2} \right)^{1/3}. \quad (A9)$$

For the values of the parameters considered above, we find a minimum contact radius $\mathcal{R} \approx 21$ Å.

¹G. Binnig, H. Rohrer, Ch. Gerber, and E. Weibel, Phys. Rev. Lett. **50**, 120 (1983).

²G. Binnig, C. F. Quate, and Ch. Gerber, Phys. Rev. Lett. **56**, 930 (1986).

³J. N. Israelachvili, *Intermolecular and Surface Forces*, 2nd ed. (Academic, San Diego, 1991), p. 112.

⁴H. C. Hamaker, Physica **4**, 1058 (1937).

⁵D. Sarid and V. Elings, J. Vac. Sci. Technol. B **9**, 431 (1991).

⁶H. B. G. Casimir and D. Polder, Phys. Rev. **73**, 360 (1948).

⁷G. Meyer and N. M. Amer, Appl. Phys. Lett. **53**, 1045 (1988).

⁸H. K. Wickramasinghe, J. Vac. Sci. Technol. A **8**, 363 (1990).

⁹T. R. Albrecht, P. Grütter, D. Horne, and D. Rugar, J. Appl. Phys. **69**, 668 (1991).

¹⁰D. Tabor and R. H. S. Winterton, Proc. R. Soc. London, Ser. A **312**, 435 (1969).

¹¹F. O. Goodman and N. Garcia, Phys. Rev. B **43**, 4728 (1991).

¹²H. Hertz, J. Reine Angew. Math. **92**, 156 (1881).

¹³K. L. Johnson, K. Kendall, and A. D. Roberts, Proc. R. Soc. London, Ser. A **324**, 301 (1971).

¹⁴H. G. Hansma, J. Vesenska, C. Siegler, G. Kelderman, H. Morrett, R. L. Sinsheimer, V. Elings, C. Bustamante, and P. K. Hansma, Science **256**, 1180 (1992); H. G. Hansma, R. L. Sinsheimer, M.-Q. Li, and P. K. Hansma, Nucleic Acids Research **20**, 3585 (1992).

- ¹⁵W. Zhong, G. Overney, and D. Tománek, *Europhys. Lett.* **15**, 49 (1991).
- ¹⁶N. A. Burnham, D. D. Dominguez, R. L. Mowery, and R. J. Colton, *Phys. Rev. Lett.* **64**, 1931 (1990).
- ¹⁷Park Scientific Instruments, 1171 Borregas Ave. Sunnyvale, California 94089.
- ¹⁸U. Hartmann, *Phys. Rev. B* **43**, 2404 (1991). In addition, Drexler has discussed the possibility of eliminating vdW forces by using binary mixtures to tune the dielectric properties of the medium. One potential problem is that the tip or the sample may selectively adsorb one of the components, thus hindering efforts to "tune" the properties. See K. E. Drexler, *J. Vac. Sci. Technol. B* **9**, 1394 (1991).
- ¹⁹E. M. Lifshitz, *Sov. Phys. JETP* **2**, 73 (1956).
- ²⁰B. W. Ninham and V. A. Parsegian, *Biophys. J.* **10**, 646 (1970).
- ²¹D. B. Hough and L. R. White, *Adv. Colloid Interface Sci.* **14**, 3 (1980).
- ²²J. N. Israelachvili, Ref. 3, p. 184.
- ²³In viscous fluids such as ethylene glycol, the "snap" of the tip from its far field equilibrium to contact takes a measurable amount of time. In less-viscous fluids, the snap takes less time than the sampling interval of our electronics (2.5×10^{-3} s for the rate chosen).
- ²⁴*Smithsonian Physical Tables*, 9th ed., edited by W. E. Forsythe (Smithsonian Institution, Washington, 1959).
- ²⁵*Handbook of Optical Constants of Solids*, edited by E. D. Palik (Academic, Orlando, 1985).
- ²⁶J. Mahanty and B. W. Ninham, *Dispersion Forces* (Academic, New York, 1976), p. 74.
- ²⁷*Lange's Handbook of Chemistry*, 12th ed., edited by J. A. Dean (McGraw-Hill, New York, 1979).
- ²⁸*Handbook of Chemistry and Physics*, 53rd ed., edited by R. C. Weast (Chemical Rubber Company, Cleveland, 1972).
- ²⁹S. J. O'Shea and M. E. Welland, *Appl. Phys. Lett.* **60**, 2356 (1992).
- ³⁰J. L. Hutter and J. Bechhoefer (unpublished).
- ³¹Solvation forces are forces between bodies in a liquid which exist for separations comparable to the size of the liquid molecules, where a continuum approach is not valid. They arise from the ordering of the molecules at the surfaces. See J. N. Israelachvili, Ref. 3, Chap. 13.
- ³²Some first steps along these lines have been taken by L. Olsson. See L. Olsson, P. Tengvall, R. Wigren, and R. Erlandsson, *Ultramicroscopy* **42-44**, 73 (1992).
- ³³J. N. Israelachvili, Ref. 3, p. 320.
- ³⁴J. N. Israelachvili, Ref. 3, p. 202.